

Photodetectors based on two-dimensional materials and organic thin-film heterojunctions

Jiayue Han(韩嘉悦), Jun Wang(王军)

Citation: Chin. Phys. B . 2019, 28(1): 017103. **doi:** 10.1088/1674-1056/28/1/017103
Journal homepage: http://cpb.iphy.ac.cn; http://iopscience.iop.org/cpb

What follows is a list of articles you may be interested in

Tuning electronic properties of the S_2/graphene heterojunction by strains from density functional theory

Jun-Hui Lei(雷军辉), Xiu-Fen Wang(王秀峰), Jian-Guo Lin(林建国)
Chin. Phys. B . 2017, 26(12): 127101. **doi:** 10.1088/1674-1056/26/12/127101

Recent progress on integrating two-dimensional materials with ferroelectrics for memory devices and photodetectors

Jianlu Wang(王建禄), Weida Hu(胡伟达)
Chin. Phys. B . 2017, 26(3): 037106. **doi:** 10.1088/1674-1056/26/3/037106

Electronegativity explanation on the efficiency-enhancing mechanism of the hybrid inorganic-organic perovskite ABX_3 from first-principles study

Qing-Yuan Chen(陈清源), Yang Huang(黄杨), Peng-Ru Huang(黄鹏儒) Tai Ma(马泰), Chao Cao(曹超), Yao He(何垚)
Chin. Phys. B . 2016, 25(2): 027104. **doi:** 10.1088/1674-1056/25/2/027104

Neutron irradiation effects on AlGaN/GaN high electron mobility transistors

L? Ling,Zhang Jin-Cheng,Xue Jun-Shuai,Ma Xiao-Hua,Zhang Wei,Bi Zhi-Wei,Zhang Yue,Hao Yue
Chin. Phys. B . 2012, 21(3): 037104. **doi:** 10.1088/1674-1056/21/3/037104

TOPICAL REVIEW — Photodetector: Materials, physics, and applications

Photodetectors based on two-dimensional materials and organic thin-film heterojunctions*

Jiayue Han(韩嘉悦)[1] and Jun Wang(王军)[1,2,†]

[1] School of Optoelectronic Science and Engineering, the University of Electronic Science and Technology of China, Chengdu 610054, China
[2] State Key Laboratory of Electronic Thin Films and Integrated Devices, University of Electronic Science and Technology of China, Chengdu 610054, China

(Received 19 September 2018; revised manuscript received 5 November 2018; published online 30 December 2018)

High-performance photodetectors are expected to open up revolutionary opportunities in many application fields, such as environment monitoring, military, optical communication and biomedical science. Combining two-dimensional materials (which have tunable optical absorption and high carrier mobility) with organic materials (which are abundant with low cost, high flexibility and large-area scalability) to form thin-film heterojunctions, high-responsivity photodetectors could be predicted with fast response speed in a wide spectra region.In this review, we give a comprehensive summary of photodetectors based on two-dimensional materials and organic thin-film heterojunctions, which includes hybrid assisted enhanced devices, single-layer enhanced devices, vertical heterojunction devices and tunable vertical heterojunction devices. We also give a systematic classification and perspectives on the future development of these types of photodetectors.

Keywords: photodetectors, two-dimensional materials, organic thin film, heterojunction

PACS: 71.20.Rv, 81.05.ue, 85.60.Gz **DOI:** 10.1088/1674-1056/28/1/017103

1. Introduction

Over the past few years, two-dimensional materials (2DMs) and their composite structure of a photoelectric detector have triggered a number of researchers' interests. In particular, the 2DM/semiconductor heterojunction photodetector is one of the important branches, and there are some highly relevant previous works showing excellent performance.[1–4] In terms of the excellent carrier transmission ability and semiconductor photoelectric conversion capability, the 2DM/semiconductor heterojunction photodetector presents unique advantages such as fast response speed, high responsivity and spectrum specificity.[5–14] Incorporating 2DMs with organic materials makes it possible to have large-scale high-performance photodetectors in the future due to the organic materials' large-area scalability, richness in variety and low-cost features.Organic molecules can be attached onto the surface of 2DMs by solution or epitaxial growth using Van der Waals (VdW) or chemistry interactions; such methods have been explored in detail to optimize the interface contact and tune the photoelectric properties of 2DMs. Therefore, we have the opportunity to properly incorporate those organic semiconductors with 2DMs for optoelectronic applications.Likewise their inorganic counterpart, hybrid 2DM/organic semiconductor heterojunctions, have been characterized and employed mainly aiming at two distinct goals: fabricating novel device architectures and changing the fundamental physical properties of 2DMs. Moreover, the compatibility of these two-material heterojunction systems brings many benefits, such as 2D atomic crystals showing flat and inert surfaces, which can be suitable for organic molecule ordered self-assembly.[15]

One of the key components of photodetectors is how to effectively convert light into electrical signals, usually a photocurrent or photovoltage, which is caused by different structures.[16,17] High-performance photodetectors show huge potential in the development of novel technologies in many application fields, such as scientific research, environment monitoring, military, optical communication, biomedical science, security checks and industrial processing control.[18–22]

In this review, we will discuss the recent progress of photodetectors based on 2DMs and organic thin-film heterojunctions. In Section 2, we will mainly review some fundamental parameters of photodetectors. In Section 3, the recent advances in organic photodetectors (OPs) will be presented. Many organic synthetic materials and typical photodetectors will be mentioned here, which will guide the fabrication and design of 2DM/organic heterojunction detectors. In Section 4, some strategies of design of 2DM/organic heterojunction photodetectors are systematically summarized and analyzed. Especially, a number of novel and representable works reported are divided into four typical parts. Finally, future prospects in 2DM/organic semiconductor heterojunction photodetector research are provided.

*Project supported by National Science Funds for Creative Research Groups of China (Grant No. 61421002).
†Corresponding author. E-mail: wjun@uestc.edu.cn
© 2019 Chinese Physical Society and IOP Publishing Ltd

2. Characterization parameters for photodetector performance

Photodetectors have significant importance in environment monitoring, military, communication and so on. To accurately evaluate the performance of photodetectors, several characterization parameters will be given to make a clear comparison of various photodetectors.

Photoelectric detection mainly consists of three processes: light harvesting, exciton separation and charge carrier transport, by which a photodetector can convert a light signal into an electrical signal. In order to distinguish diverse of this conversion,the external quantum efficiency (EQE) presents the photon–electron conversion efficiency and is described by

$$\mathrm{EQE} = \frac{I_{\mathrm{ph}}}{q\varphi} = \frac{h\nu}{q}\frac{I_{\mathrm{ph}}}{P}, \tag{1}$$

where $h\nu$ is the energy of the incident photon, I_{ph} is the photocurrent, q is the elementary electron charge, φ is the photon flux and P is the power of the incident light. To further understand the detector's photoresponse ability, a more direct figure of merit named responsivity (R) is presented as follows:

$$R = \frac{I_{\mathrm{ph}}}{p}, \tag{2}$$

where R has the unit of A/W. Another core parameter of the photodetector allows us to distinguish between the noise and the light response capability, which is called detectivity (D^*):

$$D^* = \frac{\sqrt{A\Delta f}}{\mathrm{NEP}} \quad \text{or,} \quad D^* = \frac{I_{\mathrm{ph}}}{p_{\mathrm{i}}\sqrt{2qI_{\mathrm{dark}}}}, \tag{3}$$

where p_{i} is the light intensity, I_{dark} is the dark current, A is the active area, Δf is the detection bandwidth and NEP is the noise-equivalent power. The temporal response time is an important parameter to describe the time-motivated photocurrent changing costs when the light is shed on a photodetector. The response and recover process is expressed as the rise (τ_{rise}) and decay (τ_{decay}) times. The trap state like the defect makes it possible for conductive high gain (G) device;photoconductive gain can be determined as follows:

$$G = \tau_{\mathrm{life}}/\tau_{\mathrm{transit}}, \tag{4}$$

where τ_{life} is the carrier lifetime, τ_{transit} is the short drift transit time and can be given as $\tau_{\mathrm{transit}} = L^2/\mu V_{\mathrm{bias}}$.

One more important operating parameter of a photodetector, response time, is extremely influenced by interfacial carrier transport and electrode collection, which are defined as the rising time measured from 10%/90% and the falling time from 90%/10% of the net photocurrent.

3. Recent advances in OPs

OPs can be used in biomedical science, education, environmental monitoring, optical communication, computer vision and sensory imaging.[23,24] The development of organic solar cells (OSCs) and OPs always promotes each other. In principle, both OSCs and OPs aim at converting absorbed incoming light into an efficient electrical signal. Some progress has been made in the OSC field.[25–27] Compared with the small exciton binding energy of inorganic materials,[28,29] the higher exciton binding energy of the organic semiconductor is in the range of 0.3–1 eV.[30,31] Therefore, the organic bulk or planar heterojunction (donor–acceptor chromophore) are considered to realize efficient exciton dissociation.[32] Under an efficient electric field, a photo-generated exciton can dissociate until finally collected by the electrode. On the different bases of application value, distinct design ideas emerge.

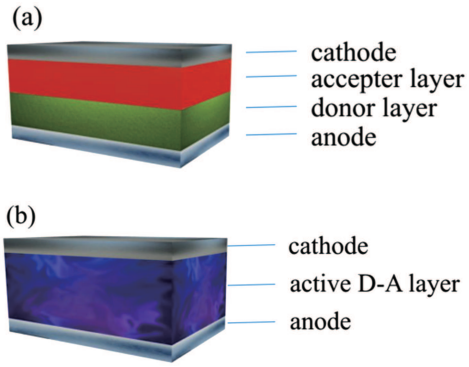


Fig. 1. Donor–acceptor heterojunction architectures. (a) Planar heterojunction (PHJ) configuration. (b) Bulk heterojunction (BHJ) configuration.

In 1981, Kudo and Moriizumi demonstrated the first OP device,[33] and at this moment, researchers realized that OPs can be fabricated by organic materials without the need for additional filters to achieve a selective response at specific wavelengths of light.

With the rapid development of polymer detectors, small organic molecule detectors have been widely discussed.[34–37]It is crucial to exploit small-molecule OPs with a structure that contains PHJs as depicted in Fig. 1(a). PHJ devices provide several advantages due to their layer-distinct structure, high carrier mobility, easy processing (thermal evaporation), richness in nature, easy purification and synthetic reproducibility.[1,38,39] These remarkable advances provide PHJ materials a potential future for OP applications with high performance.

The series of phthalocyanine small-molecule materials as a donor layer incorporating small-molecule fullerene acceptors C_{60} or C_{70} has been investigated for decades. Some of them, including lead phthalocyanine (PbPc) or zinc phthalocyanine (ZnPc), have an absorption spectrum that is extended to the near-infrared region, which can be used to design excellent OPs.[40,41]Moreover, porphyrin-basedis also popular as a donor in OPs.[42] Qi *et al.* fabricated novel small-molecule OPs based on donor–acceptor–donor type M1 and M2, in

which the electron donor was bis(2-thienyl)-N-alkylpyrrole and the acceptor was thieno [3,4-b]thiadiazole.[43] On the basic of these two new compounds, the OPs present high detectivity (D^*) of 5.0×10^{11} J at 800 nm with a bias of -0.1 V. The diffusion length of the exciton is relatively shorter than the optical absorption length resulting in a lower EQE. To settle this issue, a strategy of multiple and highly folded interfaces has sparked a wide interest in designing organic multilayer photodetectors.[44,45] Therefore, the development of a small-molecule photodetector will facilitate the progress of fabricating 2DM/organic heterojunction photodetectors.

In recent years, polymer photodetectors have attracted much attention due to their potential for fabrication on flexible substrates by low-cost methods. As narrow band gap-conjugated polymers with a broad absorption spectrum and response can be designed and synthesized, detectors based on these polymers have a continuous wideband working region. To possibly enlarge the contact area of the D–A interfaces (as shown in Fig. 1(b)), which enhances the possibility of exciton dissociation, the BHJ concept was proposed for the first time in 1995 in polymer–fullerene and polymer–polymer systems.[46,47]In addition, similar to polymer OSCs, the structures of polymer photodetectors are also based on BHJ,[42,48–54] where the active layer is prepared by blending donor–acceptor. Due to the ultrafast charge transfer at the interface between the polymer and fullerene, the polymer detector has the characteristics of fast response and high sensitivity.[1,39] These advances are a major breakthrough in the field of polymer near-infrared photoelectric detectors. With the design and synthesis of new narrow band gap polymer near-infrared materials and the urgent demand for low-cost, portable and widely used photoelectric detectors, this field is believed to be booming. Polymer OPs will also pave the way for 2DM/OPs.

As one of the popular materials of recent times, organic–inorganic hybrid perovskites (such as $CH_3NH_3PbX_3$, $X = $ Cl, Br, I) have recently attracted great attention due to their unique and excellent performance in photoelectricity.[55,56] Hu *et al.* reported their first perovskite photodetector with a broadband response in 2014.[57] This perovskite photodetector shows high responsivity of 3.49 A/W and 0.0367 A/W at a voltage bias of 3 V, and EQEs of 1.19×10^3% and 5.84% at 365 nm and 780 nm, respectively. Dou *et al.* demonstrated a vertical perovskite device with an OSC design.[58] The device shows a broadband photoresponse from 300 to 800 nm and a high EQE of 80%, with a D^* of 10^{14} J from 350 to 750 nm. Its excellent photoelectric properties will pave the way for designing 2DM/perovskite devices.

In recent years, nonfullerene acceptor (NFA)-based OPs have been studied preliminarily.[59,60] There are two main purposes for substituting fullerenes: i) The weak absorption in the first excited state of fullerenes (C_{60}-based); ii) The band gap can be hard to modify.[61,62] Over the years, a lot of exciting and remarkable progress on NFAs has provided effective methods to overcome these weaknesses.[63–69] These issues seriously affect the performance of the OPs. Gasparini *et al.* showed a solution-processed OP using a nonfullerene electron acceptor (IDTBR) blending with P3HT.[60] A relatively high responsivity of 0.42 A/W and an EQE of 69% are depicted at 755 nm. Wang *et al.* fabricated a nonfullerene ultraviolet-visible OP with a D^* of 4.9×10^{10} J at 350 nm. The NFA-based OPs still have a long way to go. These novel materials will have a profound impact on the design of 2DM/organic heterojunction photodetectors.

4. Some design strategies of 2DM/organic heterojunction photodetectors

In recent years, 2DM/organic heterojunction detectors have been widely studied, from which a large number of novel structures have emerged. We prefer to classify 2DM/organic heterojunction photodetectors into four categories, namely single-layer enhanced devices, hybrid assisted enhanced devices, VdW vertical heterojunction devices and tunable vertical heterojunction devices (Fig. 2). At the beginning, two typical 2DM/OPs based on a photogating effect will be introduced with different structure enhanced layers. This type of photoconductive photodetector will present a characteristic performance of high gain, limited response time and narrow detection spectrum. Then, the

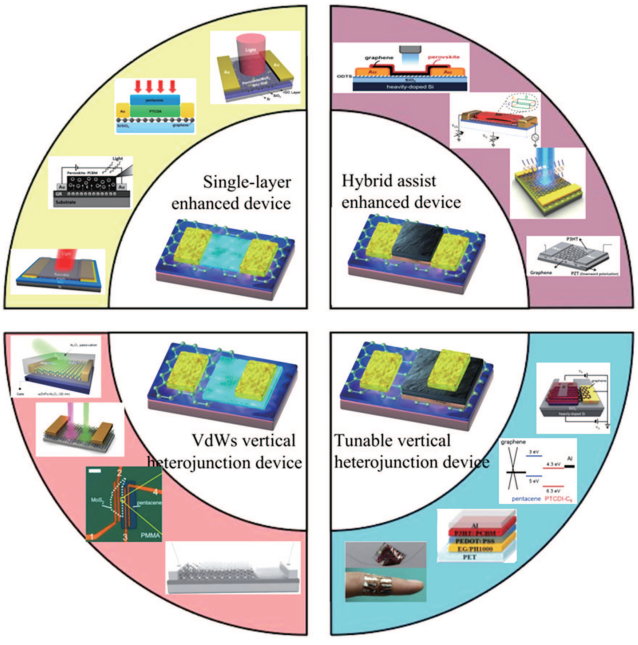


Fig. 2. Four classifications of photodetectors based on 2DMs and organic thin-film heterojunctions.

VdW heterostructures, especially p–n junction photodetectors, will exploit a new optoelectronic property, which displays a relatively faster response time than photoconductive photodetectors. In the last part, we discuss some of the novel untraditional structures of 2DM/OPs.

4.1. 2DM/organic single-layer enhanced photoconductive photodetector

Over the recent years, 2DMs are widely used in photoconductive photodetectors due to their high mobility and low state density. These 2DMs provide a novel platform for exploring localized field-enhanced photoconductive photodetectors. The photogating effect always plays an important role in 2DM hybrid structure devices. However, limited by the thickness, the 2DMs need incorporating with thin-film semiconductors to enhance the photoresponse. The photogating effect could be simply attributed to the extended photo-generated carrier lifetime caused by defects and impurities or artificially designed hybrid multilayer structures.[70] The carrier traps trap one kind of photo-generated carrier to cause a spatial separation, which produces an electrostatic field to modulate the 2DM's channel conductance. Moreover, the photogating photodetectors present high gain (G), limited response time and a narrow detection spectrum. The carrier traps promote the carrier lifetime (τ_{life}) to be relatively long. Therefore, long τ_{life} makes high gain ($G = \tau_{\text{life}}/\tau_{\text{transit}}$, τ_{transit} is the carrier transit time) at the cost of the response time.[71,72]

In this part, we will present some typical 2DM/organic hybrid photoconductive photodetectors, especially the single-layer type with 2DMs. As mentioned above, VdW heterostructures assembled by vertically stacked organic–inorganic 2DMs have attracted great interest in recent years. In addition to the previously mentioned VdW method for p–n junctions, few-layer high-gain photoconductive devices can also be epitaxially grown.

Liu *et al.* exhibited their epitaxially grown small-molecule C_8-BTBT on top of graphene with a VdW approach. The C_8-BTBT/graphene hybrid phototransistors can demonstrate a photoresponsivity of 4.76×10^5 A/W, a gain larger than 10^8.[73] Moreover, they can precisely control the number of layers of small organic molecules, which allows the device to maximize device performance (presented in Fig. 3(a)).

The solution process is another method to fabricate high-gain devices, including 3D thin film, single crystalline, 0D quantum dots (QDs) and organic–inorganic hybrid lead halide perovskites. Over the past few years, methylammonium lead halide ($CH_3NH_3PbX_3$) perovskites with their extreme optoelectronic properties have caused great concern, and are usually regarded as an active layer in photovoltaic cell applications.[74,75]To enhance the light absorption of graphene, Lee *et al.* combined graphene with ($CH_3NH_3PbX_3$) perovskites via a solution process with high photoresponsivity and the EQE was 180 A/W and 5×10^4% under a relatively low visible illumination power, which is attributed to the efficient charge transfer from the graphene to the perovskite (see Figs. 3(b) and 3(c)).[76]

0D perovskite QDs, whose three dimensions are limited in the nanoscale, possess unique photoelectric properties, a high light absorption coefficient and solution-processed advantages. The band gaps of QDs could be easily regulated by various dot sizes and components.[77] Pan *et al.* exhibited a photodetector based on $FAPbBr_3$ perovskite QD–graphene hybrid as shown in Fig. 4(a) with a high photoresponse of 1.15×10^5 A/W (EQE of 3.42×10^7%), which contains a broad spectral photoresponse ranging from 405 to 980 nm (Fig. 4(b)).[78]

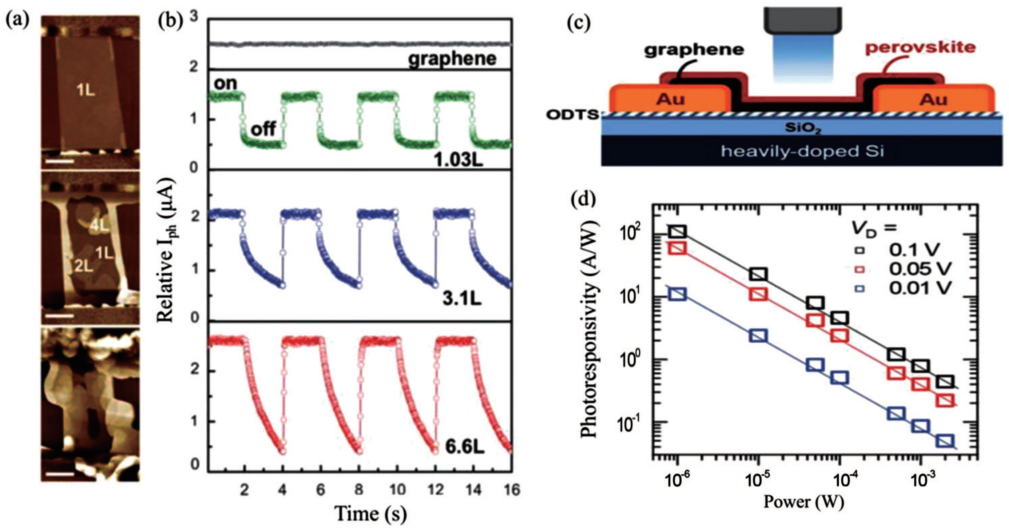


Fig. 3. (a) Atomic force microscopy (AFM)images of different increasing C_8-BTBT thickness.[73] (b) The photocurrent response of the devices in left AFM image at the laser power density of 7000 μW·cm^{-2} and $V_{ds} = 0.1$ V, V_g–$V_0 = 10$ V.[73] (c) 3D schematic view of graphene/perovskite($CH_3NH_3PbX_3$) photodetector.[76] (d) Responsivity of device at different drain voltages as a function of the illumination power.[76]

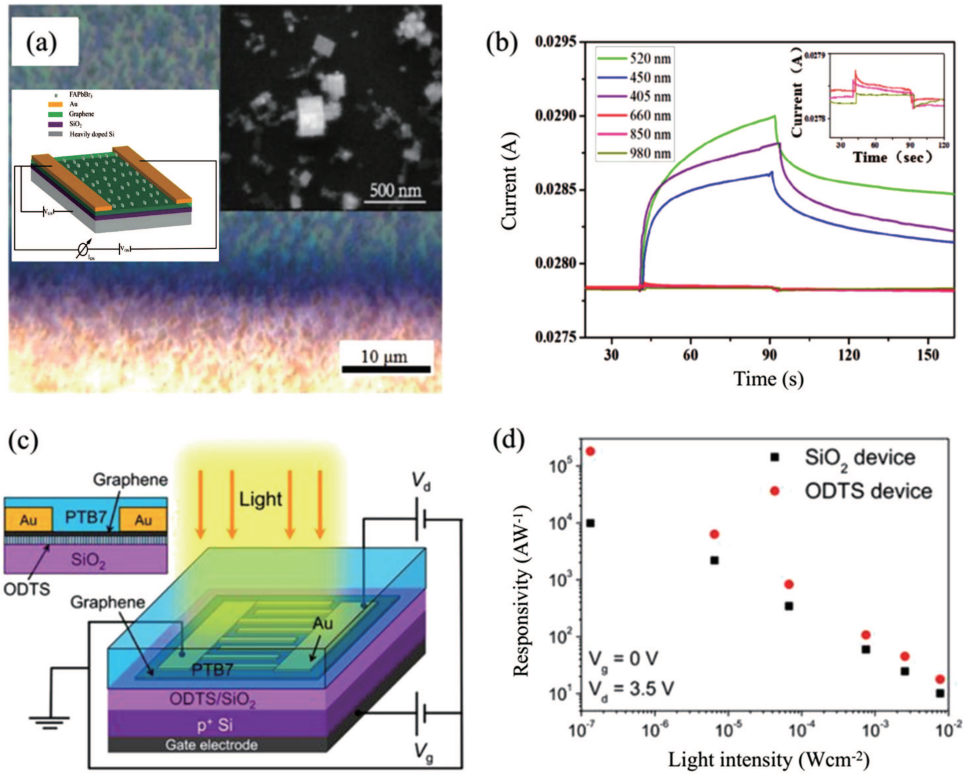


Fig. 4. (a) Diagram of $FAPbBr_3$ QD/graphene photodetector, and optical and SEM image of the $FAPbBr_3$ QDs.[78] (b) Time-dependent responsivity characteristics of the photodetector. The channel length is 80 μm.[78] (c) 3D schematic view of graphene-PTB7 hybrid photodetector.[79] (d) The responsivities of the SiO_2 and ODTSdevices as a function of power density at a drain voltage of 3.5 V and without gate voltage.[79]

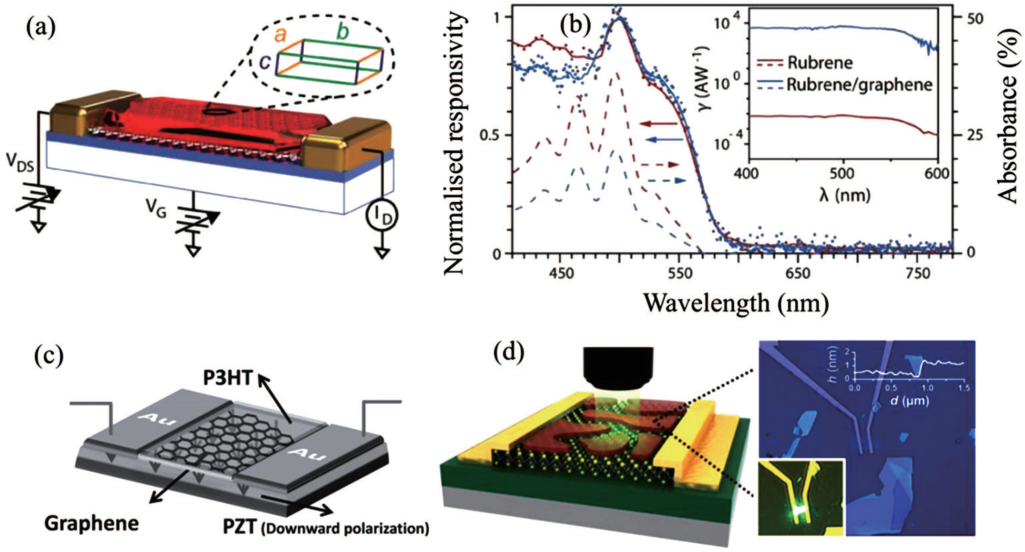


Fig. 5. (a) 3D schematic view of graphene–rubrene hybrid photodetector.[81] (b) Responsivity spectra of rubrene (red) and rubrene–graphene (blue) photodetector.[81] (c) Schematic diagram of graphene–P3HT device with a substrate of PZT.[83] (d) 3D schematic view of the single-layer MoS_2 photodetectors treated with organic dye molecules (R6 G) and optical microscopy images of the R6 G-sensitized MoS_2 photodetectors.[84]

Relying on a similar device structure, the graphene–polymer semiconductor PTB7 hybrid photodetector can show responsivity of about 10^4 A/W and a fast response time of 7.8 ms (as displayed in Fig. 4(c)). Moreover, an ODTS functionalization substrate was used to effectively remove surface traps and charged impurities of graphene, which can further optimize responsivity up to 10^5 A/W (see Fig. 4(d)).[79] The special organic chlorophyll is remarkably stable as a biomaterial for fabricating a low-cost phototransistor. Chen *et al.* showed the superior performance of graphene–chlorophyll hybrid phototransistors, with a high gain of 10^6 electrons per photon and a high responsivity of 10^6 A/W, which can be attributed to the excellent light absorbing and photogating effects of chlorophyll molecules.[80] Single crystalline organic also exhibits great potential in designing high-gain phototransistors. Jones *et al.* fabricated an ultrahigh-performance

graphene/rubrene phototransistors (see Fig. 5(a)) with a detectivity of 9×10^{11} J in broadband, which approaches the detectivity of single-photon detectors (see Fig. 5(b)).[81]

Wang *et al.* found that the unique performance of the P(VDF-TrFE)-driven MoS_2 photodetector was significantly enhanced compared to pure MoS_2,[82] and the appropriate substrate can optimize the device performance. In this device, by use of the remnant polarization of P(VDF-TrFE), the dark current of the MoS_2 channel device is depressed, which enhances the performance of the device. The idea of residual polarization mentioned above has been brought in graphene organic heterojunction devices. By properly orienting the polarization of piezoelectric (PZT) substrate, the graphene-P3HT photodetectors enhance their photocurrents by about ten times compared to SiO_2 substrate and extend the response spectrum, due to the more effective separation of photo-generated electron–hole pairs promoted by the PZT substrate (see Fig. 5(c)).[83]

Besides graphene, other 2DMs such as MoS_2 can also be incorporated with organic semiconductors. High-performance dye-sensitized MoS_2 photodetectors combine single-layer MoS_2 with rhodamine 6 G organic dye molecules (see Fig. 5(d)). The hybrid photodetectors demonstrate a responsivity of 1.17 A/W, a detectivity of 1.5×10^7 J and a spectral coverage from 405 to 980 nm.[84] In general, the high-gain photoconductive device can amplify light signals at ultralow light levels at the cost of the response time and on/off ratio. These 2DM/organic hybrids mentioned above pave the way for implementing low-cost, flexible, high-performance photodetectors in the future.

4.2. Organic hybrid assisted enhanced photoconductive photodetector

The OP of the planar heterojunction device refers to the contact surface of two materials: the donor–acceptor plane. The general selection pair organic semiconductor materials with large absorption coefficients in the waveband to detect light are ideal as electron donors.It is desirable to select an electron transport material with a high absorption coefficient for the light to be detected, and the energy level matching of the donor/acceptor should be considered.

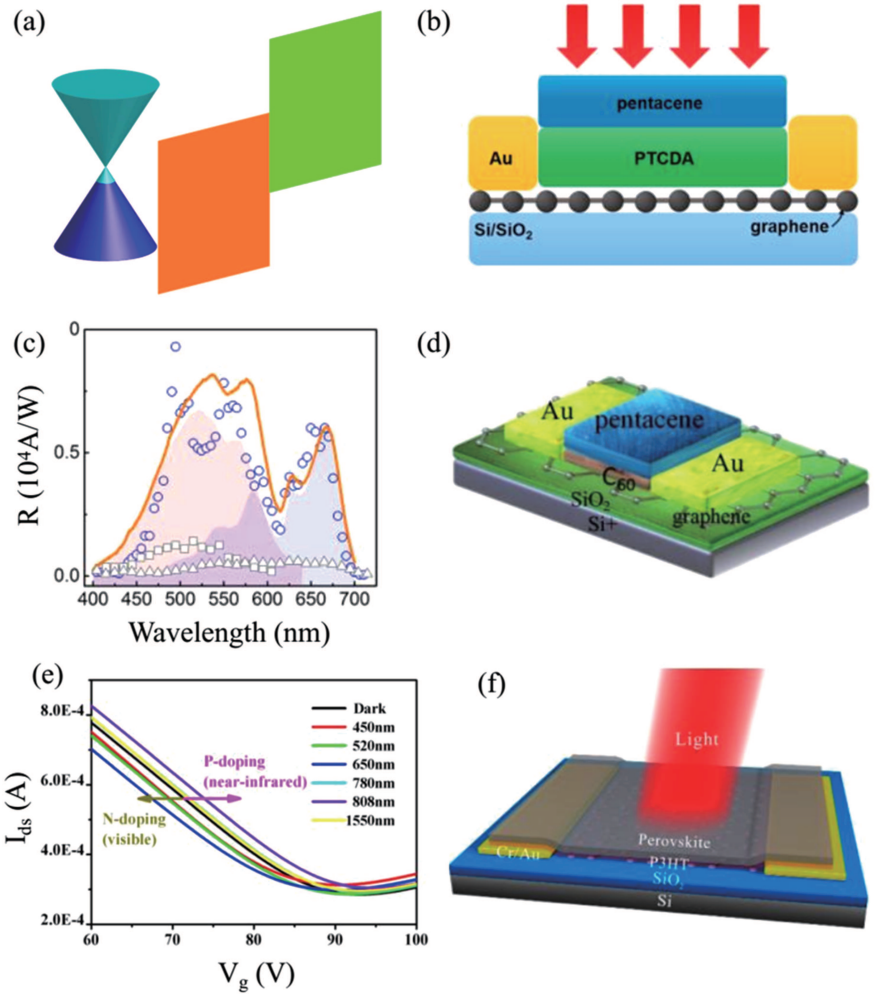


Fig. 6. (a) Schematic diagram of the enhanced type-II heterojunction on 2DM (such as graphene) photoconductive photodetector. (b) Diagram of graphene/PTCDA/pentacene phototransistor structure. (c) Photoresponsivity of graphene/PTCDA/pentacene and control devices. Blue circles: the average thickness of PTCDA/pentacene and coverage of pentacene is 4 nm/1.3 L/82%) and control devices (gray squares: graphene/PTCDA; gray triangles: graphene/pentacene) at the laser power of 100 μW. (d) Diagram of graphene/C_{60}/pentacene phototransistor structure.[88] (e) The transfer characteristic curve under illumination and in the dark.[88] (f) 3D schematic view of the graphene/P3HT/perovskite vertical heterojunction phototransistor.[85]

The heterojunctions of single-layer organic small molecules and polymers with 2DMs especially in photoconductive devices have inferior performance due to the weak interaction between interfaces. Therefore, a novel strategy for enhancing the photoresponse performance is by incorporating bulk or multilayer heterojunctions in 2DMs.[85–87] Moreover, for decreasing the recombination of photo-generated electron–hole pairs, the type-II heterojunction meets the requirements (Fig. 6(a)). The type-II PHJ or BHJ can establish an effective and strong built-in electric field, which enables the photo-generated carriers to be effectively separated, and selects one kind of carrier to be trapped, and another to inject into 2DMs to generate corresponding responses. This structure can generate higher gain than a single enhanced layer, improving the photoresponsivity and external quantum efficiency of devices and expanding the spectrum.

In general, the thickness of the multilayer should be less than the exciton diffusion length, especially the layer close to the 2DM, for obtaining the best charge separation efficiency, which is almost in the order of 5–10 nm. Chen *et al.* fabricated a graphene phototransistor by combining a PHJ multilayer (PTCDA/pentacene) to enhance the performance (see Fig. 6(b)). Compared with single-layer organic/graphene control devices, the graphene/PTCDA/pentacene device shows a ten-fold improvement in responsivity reaching 10^5 A/W over a spectrum band of 400–700 nm (see Fig. 6(c)). The graphene/PTCDA/pentacene response time can be modulated as low as 28 μs, which is the best in this type of photodetectors. We recently investigated a graphene phototransistor incorporating another p–n junction C_{60}/pentacene(see Fig. 7(e)). We demonstrated a bi-directional photoresponse as shown in Fig. 7(f) with the highest responsivity of 9173 A/W.[88]

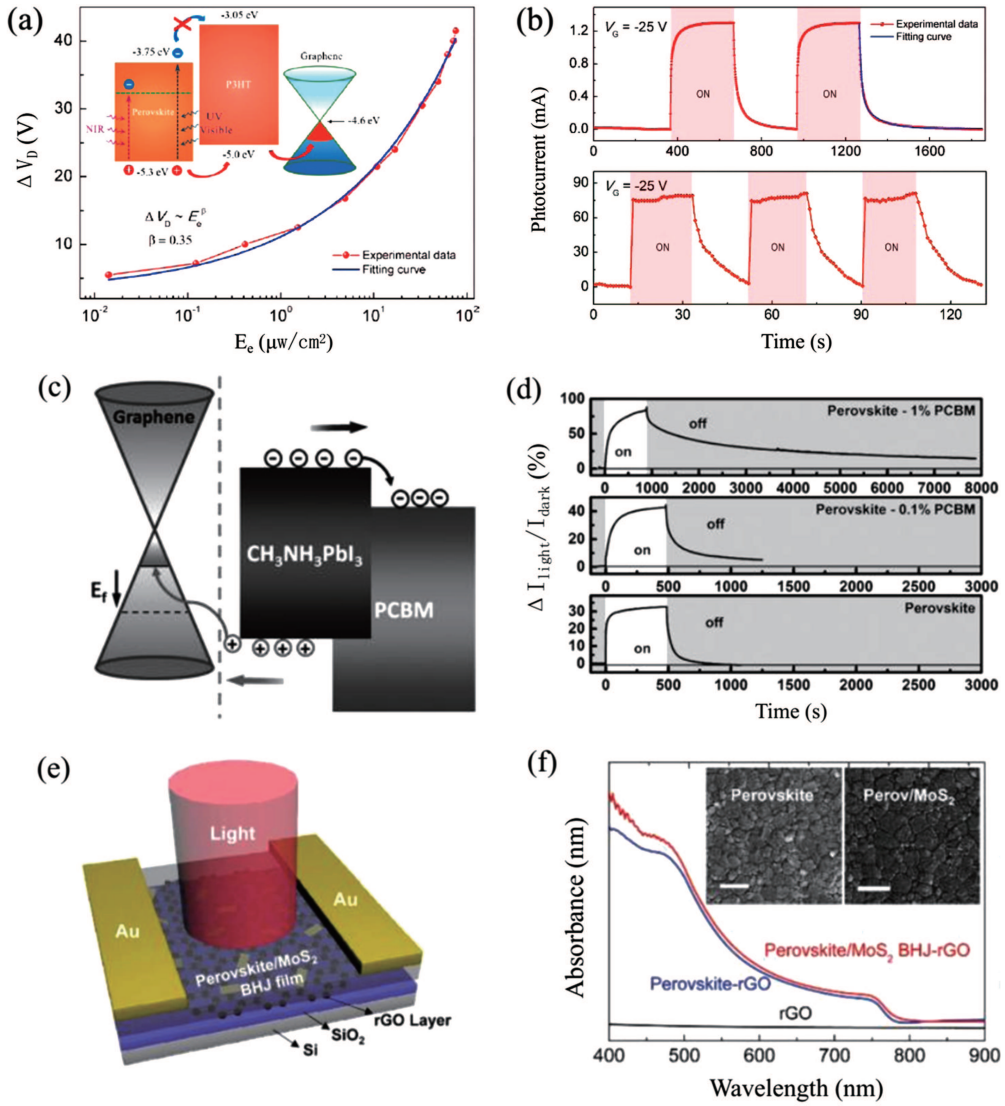


Fig. 7. (a) Shift of the Dirac point V_d as a function of the illuminating power density on the photodetector.[85] (b) The photocurrent of the photodetector under near-infrared illumination at $V_G = -15$ V, $V_{DS} = 0.05$ V.[85] (c) The energy band diagram of the graphene/PCBM/perovskite heterojunction photodetectors.[87] (d) The time-dependent measurement of the device with different PCBM concentrations at the wavelength of 500 nm.[87] (e) 3D schematic view of perovskite/MoS_2 BHJ on a reduced graphene oxidelayer.[86] (f) Absorption spectra and SEM image of device.[86]

However, unlike organic small molecules with their easy-to-obtain ultrathin layer, solution-processed polymers or perovskite can only produce a thicker BHJ.By the similar mechanism that transfers only photo-generated holes from perovskite to graphene, and electrons trapped in another material under the illumination.[85–87]Two groups of researchers have combined perovskite with an organic semiconductor to form a BHJ-enhanced layer by solution-processed spin onto a graphene surface.[85,87] By selecting electrons trapping to enhance the responsivity of device, which reach highest 4.3×10^{9} A/W in $CH_3NH_3PbI_3$-P3HT bulk heterojunction (Fig. 6(d)).By increasing the illuminated light power intensity, the shift of the Dirac point V_D (ΔV_D) is increased, as shown in Fig. 6(f). Further measurement under near-infrared illumination is depicted in Fig. 6(f).[85] Moreover, the device also demonstrates a broadband wavelength response from ultraviolet to near-infrared. Therefore, to promote the responsivity of the device, some strategies should be taken into consideration: (i) to build an effective electric field in the photoactive layer (to form a type-II heterojunction); (ii) to select one type photo-generated of the carriers trapping and another into graphene;(iii) to prolong the trapping time (equal to the lifetime) of the selected type of carriers within the photoactive layer. Liang *et al.* exhibited that their $CH_3NH_3PbI_3$-PCBM bulk heterojunction on graphene can optimize trapping time by regulating the concentration of PCBM in perovskite to enhance the responsivity as shown in Fig. 7(a).[87] They depicted that trap times with a wide range of de-trapping times exist, and the increasing falling times obtained from Fig. 7(b) exhibited for the increasing concentration of PCBM devices.They show that a perovskite with 1% PCBM photodetector has a photoresponsivity of 8×10^{5} A/W, which is about 30 times larger compared with the perovskite-only device.

In the latest work, the researchers use 2DMs instead of semiconductors as the trapped carrier material. In Fig. 7(c), Peng *et al.* demonstrated a BHJ film photodetector composed of perovskite $CH_3NH_3PbI_3$ film and MoS_2 nanoflakes on graphene.[86] Similar to the response mechanism described above, the photodetector of perovskite/MoS_2 BHJ exhibits nearly five times enhanced responsivity (1.08×10^{4} A/W), detectivity (4.28×10^{13} J), and an EQE of 2.0×10^{6}% (Fig. 7(d)).

We believe that the use of a BHJ or bilayer on the 2DMs can be a novel strategy for optimizing the photoresponsivity of sensitizer/2DM photodetectors for highly sensitive detection.

4.3. VdW vertical hybrid junction photodetector

VdW heterostructures assembled by vertically stacked inorganic 2DMs provide a fantastic platform to create novel device architectures and exploit new optoelectronic properties. The incorporation of 2DMs with organic molecules holds an immense potential for fabricating superior photodetectors. The p–n junctions are essential building blocks for light-emitting diodes, transistors, photodiodes and solar cells.[89] Molecular beam epitaxy provides a feasible way to create a high-quality heterojunction and VdW heterojunction opens up the opportunity to stack different materials without consideration of lattice match required.[90–93]In contrast to 2DM VdW heterostructures, 2DM/organic heterojunctions can realize large-scale, low-cost, high-mobility, efficient and fast photodetection, benefiting from the excellent properties of organic materials.

In recent years, VdW heterostructures have shown many fascinating physical properties, especially that its p–n junctions have always integrated 2DMs with mostly inorganic materials such as MoS_2/WSe_2,[94–96] MoS_2/black phosphorus,[97] WSe_2/carbon nanotubes[98] and graphene/carbon nanotubes.[99]

The recent advance of a wide variety of 2DMs has opened new opportunities for the fabrication of 'all 2D' VdW heterostructure devices.[98,100,101] The photodetectors exploit the semiconducting nature of certain organic molecules and 2DMs, where the 2DM/organic interface plays an irreplaceable role in determining the device performance. However, some preliminary studies have focused on the issue that a clear understanding of the charge transport process across the interface between organic and 2DMs is still lacking.[102,103]In Fig. 8(a), Jariwala *et al.* exhibited a p–n heterojunction based on pentacene and MoS_2, then investigated the electronic and optoelectronic device by direct charge transport measurements.[104] The current–voltage characteristics of p–n junctions without V_G in the dark and under light illumination are shown in Fig. 8(b). As a result, the open circuit voltage and photovoltaic measurement suggest that the MoS_2/pentacene p–n junction can be an alternative nonfullerene acceptor–donor system for organic photovoltaics and a prospect for photodetectors.

Due to its intrinsic n-type 2DM,[105,106] MoS_2 can be incorporated with another p-type organic material to fabricate the p–n heterojunctions.

By introducing ZnPc molecules onto the surface of MoS_2, the ZnPc/MoS_2 VdW heterojunction presents a great enhancement, revealing a steep photocurrent rise and decay compared to the bare MoS_2 as shown in (Fig. 8(c)).[107] Furthermore, for improving the contact metal electrodes[108] and the dielectric environments, researchers integrated an Al_2O_3 passivation layer onto the device as shown in Fig. 8(d). The device finally presents an optimized performance with a photoresponsivity of 1.4×10^{4} A/W as depicted in Fig. 8(e), and a detectivity of 10^{11} J at a 40 V gate bias and light intensity of 0.07 mW/cm^2. For future photodetector design, they render a new strategy to

realize a balanced optimization performance device by methods such as dielectric passivation and gate modulation. We think this idea may provide a new method for an overall increase in the optoelectronic performances of 2DM/organic heterojunctions in photodetection in the future.

In Figs. 9(a) and 9(b), coupling MoS_2 with graphitic carbon nitride (g-C_3N_4) can produce a promising UV-visible broadband photodetector.[109] By modulating the g-C_3N_4/MoS_2 concentration up to a 5:5 ratio, 4 A/W and 4×10^{11} J with a fast response time of 50 ms can be achieved (see Fig. 9(c)). In the g-C_3N_4/MoS_2 N–N heterostructure, the built-in electric field suppresses the dark current of the device and allows a broadband photodetection from 270 to 700 nm.

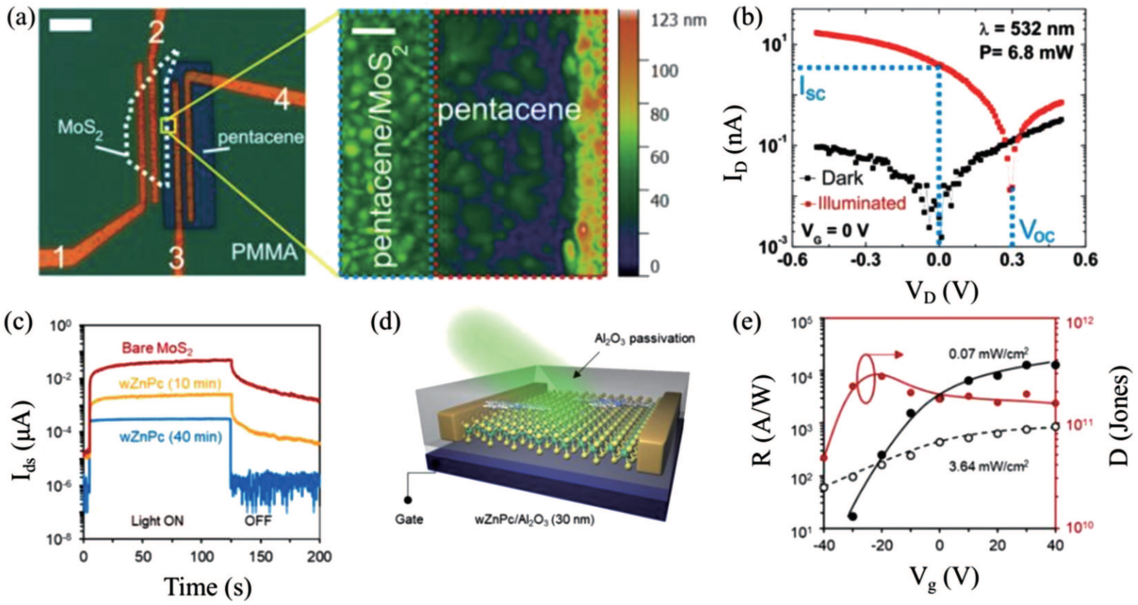


Fig. 8. (a) Optical micrograph of a representative MoS_2/pentacene p–n junction (left panel, scale bar is 10 μm). The AFM image of the MoS_2/pentacene p–n junction area (right panel, scale bar is 500 nm).[104] (b) The current–voltage characteristics of p–n junctions without V_G in the dark and under light illumination.[104] (c) The time-dependent photoresponse measurement of the MoS_2 device and MoS_2 with various ZnPc treatments.[107] (d) The diagram of MoS_2/ZnPc with an Al_2O_3 passivation layer photodetector structure.[107] (e) Gate-modulated responsivity and detectivity of the MoS_2/ZnPc photodetector with Al_2O_3 passivation at a power intensity of 0.07 and 3.64 mW/cm^2.[107]

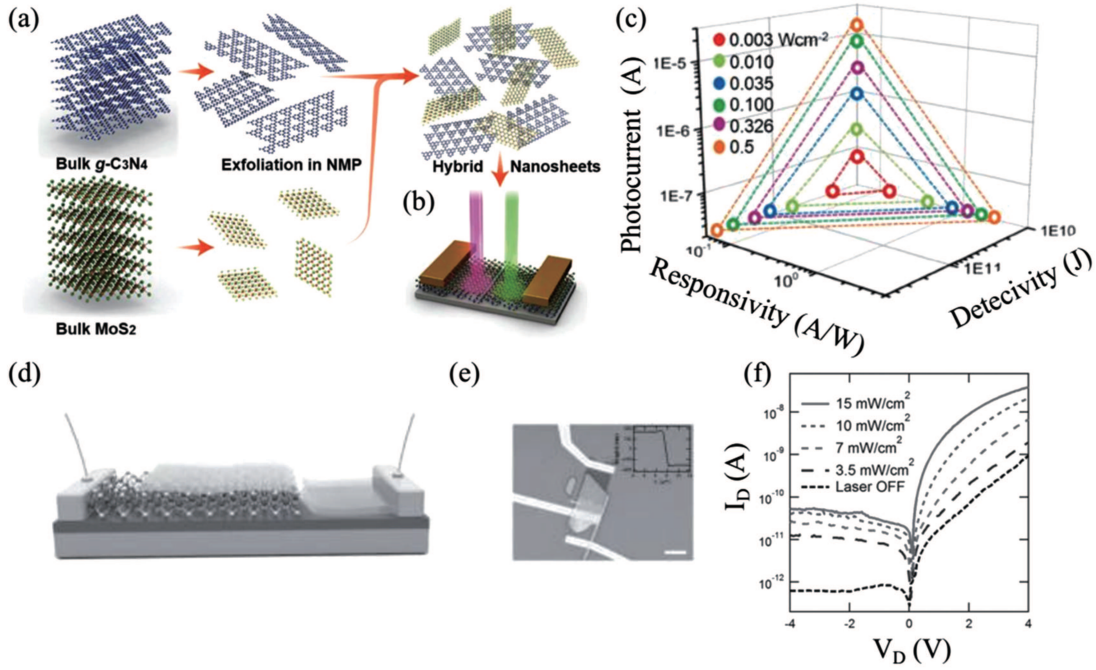


Fig. 9. (a) 3D schematic diagram and fabrication process of MoS_2 and g-C_3N_4 hybrid dispersions.[109] (b) Schematic diagram of exfoliated MoS_2 and g-C_3N_4 heterojunction nanosheets under illumination.[109] (c) Some important parameters in the UV region (photocurrent, responsivity and detectivity) of MoS_2/g-C_3N_4 photodetector as a function of the power density at a bias voltage of −9 V.[109] (d) 3D schematic view of MoS_2/rubrene hybrid device. (e) Optical microscopy image of MoS_2/rubrene hybrid device.[103] (f) The current–voltage characteristics under different light intensity excitation.[103]

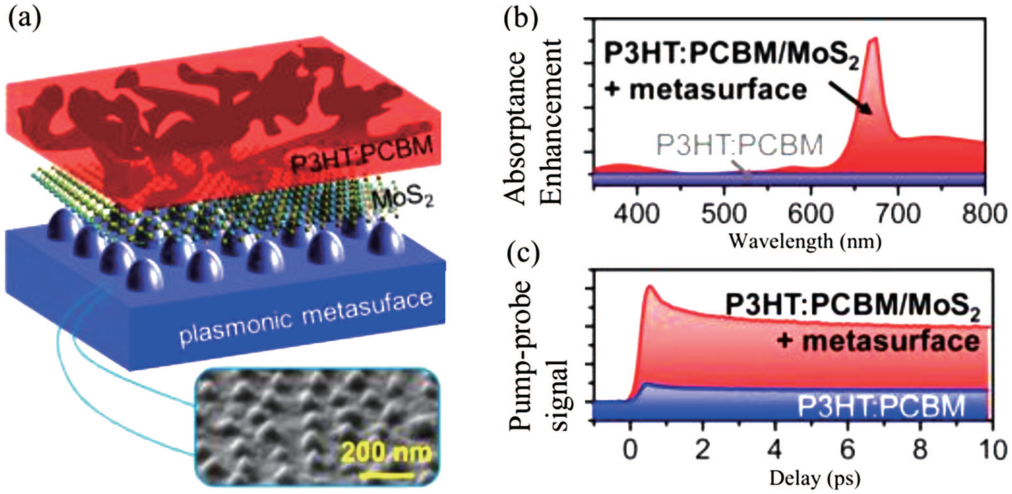


Fig. 10. (a) 3D schematic diagram of the P3HT:PCBM/MoS_2 heterojunction on the plasmonic metasurface.[113] (b) Simulated active layer absorptance of P3HT:PCBM/MoS_2 heterojunction on the plasmonic metasurface.[113] (c) Picosecond-scale transient pump-probe reflection measurements with different P3HT:PCBM and hybrid P3HT:PCBM/MoS_2 active layers.[113]

Both MoS_2 and rubrene show excellent photoelectric properties. Liu *et al.* combined MoS_2 with rubrene to fabricate a p–n junction device (see Figs. 9(d) and 9(e)), which demonstrates photoresponse properties with a responsivity of 0.51 A/W (see Fig. 9(f)), observed with a fast response time of 5 ms.[?] Moreover, the device can also be employed as a photodiode, and the most important parameter is the rectifying ratio. They realized that the device's rectifying ratio varies from 10^2 to 10^5 with the different gate voltage, which is attributed to the modulation of band alignment between MoS_2 and rubrene by the gate voltage.

In recent years, the plasmonic effect is always used in devices to generate a photo-trapping effect, which aims to enhance the light absorption of 2DMs.[110–112] Different to that described above, a disordered plasmonic metasurface aiming to increase the absorption is another way to fabricate high-performance photodetectors. In Fig. 10(d), Petoukhoff *et al.* demonstrated the influence of a plasmonic metasurface on the enhanced absorption of light in a P3HT:PCBM/MoS_2 heterojunction, which shows a new way of designing novel organic 2DM heterojunction photodetectors.[113] The enhanced absorptance and picosecond-scale transient pump-probe are displayed in Figs. 10(b) and 10(c).

Overall, 2DM/organic VdW heterojunction photodetectors have drawn a lot of attention. They provide a fantastic platform to create novel device architectures and exploit new optoelectronic properties.

4.4. Photodetector using 2DMs as tunable functional layer

Graphene and 2DMs always act as the conductive channel or light-absorbing layer. However, 2DMs, especially graphene, can be employed as a tunable functional layer due to their low density of states. The difference of the graphene source electrode doping level will have a great effect on the electrical properties, and by tuning.the work function of graphene, we may enhance the device features we need. This novel idea originates from an organic vertical field-effect transistor.[114] Moreover, Kim *et al.* used monolayer graphene as an electrode to design a novel electronic device architecture to show an unprecedented 2DM/organic phototransistor (see Figs. 11(a) and 11(b)).[115]

This device can optimize performance without using additional charge-blocking layers by tuning the graphene Fermilevel. We learn from this that tuning the Schottky barrier height between the graphene and pentacene could improve the rectification ratio of the phototransistor.Furthermore, this strategy may promote the device in two aspects: (i) suppressing the density magnitude of dark current; (ii) promoting the photocurrent of the device. Both are essential to improve the performance of a phototransistor.

In Fig. 11(a), at the reverse bias voltage the current density was obviously enhanced under illumination compared to that in the dark. When applying a negative V_G in the reverse-bias condition, the electron injection from graphene to pentacene will be suppressed compared to $V_G = 0$ (see Fig. 11(c)). Under illumination, the p–n heterojunction mainly produces electron–hole pairs in the reverse-bias condition, and the negative V_G causes a band bending of pentacene highest occupied molecular orbital.This would promote photo-generated hole transfer into the graphene electrode. Therefore, applying a negative V_G will increase the Schottky barrier height between graphene and pentacene, which will suppress the density magnitude of dark current and promote the photocurrent of the device at the same time, resulting in improved detectivity (1.26×10^9) and responsivity.[115]

To make large-area transparent electrodes of ultrathin OPs, Liu *et al.* demonstrated a novel solution process by spray-coating a hybrid ink composed of graphene and PEDOT:PSS

formulation. By employing this hybrid ink as a transparent electrode, they fabricated OPs, where P3HT:PCBM acted as an active layer as shown in Fig. 11(d). The device exhibits a great performance with a detectivity of 1.33×10^{12} J and responsivity of 0.16 A/W. The current–voltage characteristics of these photodetectors are shown in Fig. 11(e).[116]

More interestingly, this ultrathin organic flexible photodetector can be applied well in fields such as biomedicine, for example in making contact with a human finger or other body parts. The device also shows excellent stability. As depicted in Fig. 11 after 200 cycles of bending, there is no noticeable deterioration and the I_{on}/I_{off} ratio remained at the same order of magnitude. The photosensitivity of the device is also a key parameter. Figure 11(f) shows the high I_{on}/I_{off} ratio (8.4×10^4), which is close to the performance of some relative OPs.[117,118]

Different from the traditional 2DM-based hybrid photodetectors mentioned, 2DMs in this part act as electrodes or other functional layers. This type of device shows its potential for emerging flexible and novel structure devices.

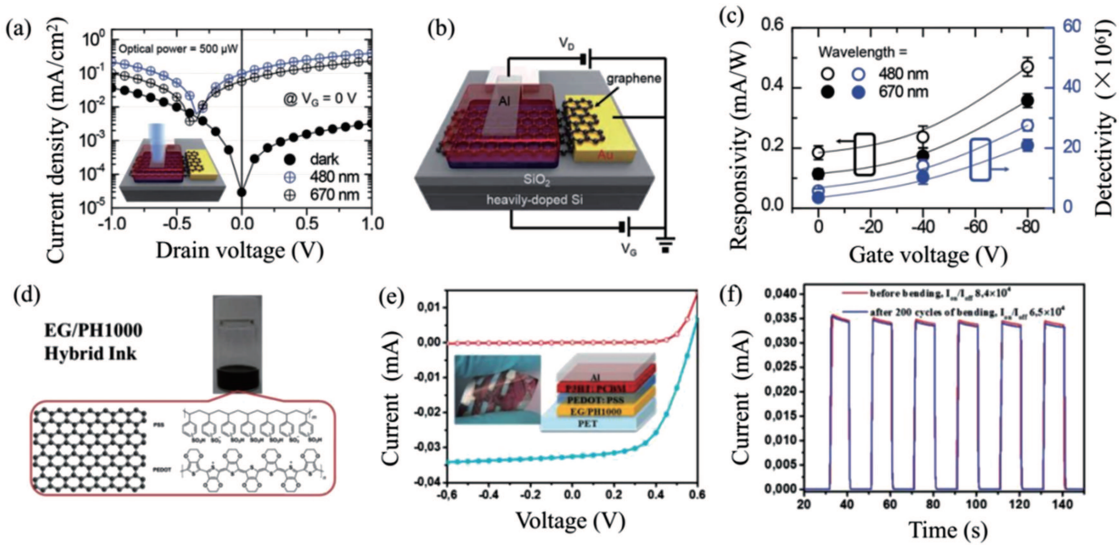


Fig. 11. (a) Current–voltage characteristics of photodiodes with graphene electrodes without V_G in the dark and under light illumination ($\lambda = 480$ and 670 nm, light power is 500 μW).[115] (b) 3D schematic view of organic vertical p–n junction photodiodes with the graphene electrode.[115] (c) Responsivity and detectivity of the device as a function of grid voltage.[115] (d) Digital image of graphene/DEPOT:PSS hybrid ink; molecular structures of graphene and PEDOT:PSS.[116] (e) The current–voltage characteristics of the photodetectors fabricated on a PET substrate.[116] (f) The on/off ratio characteristics of the graphene/PEDOT:PSS photodetector at a bias voltage of 0 V before and after the bending test.[116]

Table 1. Summary of literature data for photodetectors based on 2DMs and organic thin-film heterojunctions.

Device type	Active layer materials	Response spectrum/nm	Responsivity/A·W^{-1}	Response time/ms	EQE/%	Detectivity (D^*)	Ref.
Single-layer enhanced photodetector	Graphene/FAPbBr$_3$ QDs	405–980	1.15×10^5	58	3.42×10^7	NA	[78]
	Graphene/$CH_3NH_3PbI_3$	400–800	180	87	2×10^4	10^9	[76]
	Graphene/C8-BTBT	355	104	20	2×10^5	NA	[73]
	MoS_2/R6 G	405–980	1.17	5.1×10^{-3}	280	1.5×10^7	[84]
	Graphene/PTB7	450–800	1.8×105	7.8	NA	NA	[79]
	Graphene/P3HT	325	NA	128	NA	NA	[83]
	Graphene/chlorophyll	400–700	10^6	110	NA	NA	[80]
	Graphene/rubrene	400–600	10^7	100	3.4×10^7	9×10^{11}	[81]
Hybrid assisted enhanced photodetector	Graphene/$CH_3NH_3PbI_3$/PCBM	400–750	8×10^5	2.5×10^3	NA	NA	[87]
	Graphene/PTCDA/pentacene	400–700	10^5	0.028	9(without gain)	NA	[85]
	Graphene/$CH_3NH_3PbI_3$/MoS_2	400–750	1.08×10^4	45	2×10^6	4.28×10^{13}	[86]
	Graphene/P3HT/$CH_3NH_3PbI_3$	400–950	4.3×10^9	$> 10^3$	NA	NA	[85]
Vertical heterojunction photodetector	MoS_2/g-C_3N_4	270–700	4	50	NA	4×10^{11}	[109]
	MoS_2/rubrene	450–700	0.51	5	NA	NA	[110]
	MoS_2/ZnPc	532	1.4×10^4	8	NA	10^{11}	[107]
Tunable vertical photodetector	Graphene/pentacene/PTCDI-C8	400–670	NA	NA	NA	1.26×10^9	[115]
	Graphene/PEDOT:PSS	350–650	0.16	NA	NA	1.33×10^{12}	[116]

In conclusion, there is a great potential for incorporating organic materials with 2DMs to fabricate photoelectric detectors with excellent performance. With the continuous development of material science in the future, many novel optoelectronic devices and phenomena can be realized through the different structures and excellent properties of materials. Table 1 summarizes some reported results from photodetectors based on 2DMs and organic thin-film heterojunctions in the review. We can distinguish them by many parameters, and can see the advantages and disadvantages of various detectors. Compared with the vertical heterojunction photodetectors, the photodetectors based on photogating demonstrate a relatively high responsivity with high EQE but at the cost of detectivity. Moreover, vertical heterojunction photodetectors especially have an

advantage in detectivity. There is a balance between these parameters, and different structures will benefit from them.

5. Conclusion and perspectives

In this review, we have discussed recent advances in photodetectors based on 2DMs and organic thin-film heterojunctions, mentioning some remarkable exciting developments in this field. A large number of organic molecules or polymers collectively incorporating with 2DMs promotes the development of high-performance photodetectors. Especially, the VdW epitaxy and evaporation of organic thin film or crystal on 2DMs for electronic device applications has aroused great interest in recent research. However, in the enhanced bilayer or BHJ photoconductive photodetector field, there are still many important issues to explore. In recent years, a lot of exciting and remarkable progress in NFAs has provided effective methods to optimize OSC and OPs. Besides fullerene and traditional organic materials, nonfullerene material/2DM hybrids like perylene diimide with more remarkable advantages will draw much attention in future studies.This work opens up a versatile platform for fabricating next-generation high-performance photodetectors.

References

[1] Mueller T, Xia F and Avouris P 2010 *Nat. Photon.* **4** 297
[2] Lu H, Cumming B P and Gu M 2015 *Opt. Lett.* **40** 3647
[3] Miao J, Hu W, Guo N, Lu Z, Liu X, Liao L, Chen P, Jiang T, Wu S, Ho J C, Wang L, Chen X and Lu W 2015 *Small* **11** 936
[4] Miao J, Hu W, Jing Y, Luo W, Liao L, Pan A, Wu S, Cheng J, Chen X and Lu W 2015 *Small* **11** 2392
[5] Echtermeyer T J, Britnell L, Jasnos P K, Lombardo A, Gorbachev R V, Grigorenko A N, Geim A K, Ferrari A C and Novoselov K S 2011 *Nat. Commun.* **2** 458
[6] Kawasaki T, Sugawara K, Dobroiu A, Eto T, Kurita Y, Kojima K, Yabe Y, Sugiyama H, Watanabe T, Suemitsu T, Ryzhii V, Iwatsuki K, Fukada Y, Kani J, Terada J, Yoshimoto N, Kawahara K, Ago H and Otsuji T 2015 *Solid-State Electron.* **103** 216
[7] Vicarelli L, Vitiello M S, Coquillat D, Lombardo A, Ferrari A C, Knap W, Polini M, Pellegrini V and Tredicucci A 2012 *Nat. Mater.* **11** 865
[8] Marczewski J, Knap W, Tomaszewski D, Zaborowski M and Zagrajek P 2015 *J. Appl. Phys.* **118** 104502
[9] Furchi M, Urich A, Pospischil A, Lilley G, Unterrainer K, Detz H, Klang P, Andrews A M, Schrenk W, Strasser G and Mueller T 2012 *Nano Lett.* **12** 2773
[10] Konstantatos G, Badioli M, Gaudreau L, Osmond J, Bernechea M, Arquer F P G, Gatti F and Koppens F H 2012 *Nat. Nanotechnol.* **7** 363
[11] Kufer D, Nikitskiy I, Lasanta T, Navickaite G, Koppens F H L and Konstantatos G 2015 *Adv. Mater.* **27** 176
[12] Sun Z, liu Z, Li J, Tai G, Lau S and Yan F 2012 *Adv. Mater.* **24** 5878
[13] Fang H and Hu W 2017 *Sci. Chin.-Phys. Mech. & Astron.* **60** 027031
[14] Wang P, Liu S, Luo W, Fang H, Gong F, Guo N, Chen Z, Zou J, Huang Y, Zhou X, Wang J, Chen X, Lu W, Xiu F and Hu W 2017 *Adv. Mater.* **29** 1604439
[15] Wang Q H and Hersam M C 2009 *Nat. Chem.* **1** 206
[16] Long M, Wang P, Fang H and Hu W 2018 *Adv. Funct. Mater.* **2018** 1803807
[17] Wang J and Hu W 2017 *Chin. Phys. B* **26** 037106
[18] Gong X, Tong M, Xia Y, Cai W, Moon J S, Cao Y, Yu G, Shieh C L, Nilsson B and Heeger A J 2009 *Science* **325** 1665
[19] Vuuren R D J, Armin A, Pandey A K, Burn P L and Meredith P 2016 *Adv. Mater.* **28** 4766
[20] Baeg K J, Binda M, Natali D, Caironi M and Noh Y Y 2013 *Adv. Mater.* **25** 4267
[21] Wang H and Kim D H 2017 *Chem. Soc. Rev.* **46** 5204
[22] Arquer F P G d, Armin A, Meredith P and Sargent E 2017 *Nat. Rev. Mater.* **2** 16100
[23] Chen L, Deng J X, Kong L, Cui M, Chen R G and Zhang Z J 2015 *Chin. Phys. B* **24** 047801
[24] Yang D Z, Sun H D, Chen J S and Ma D G 2012 *Chin. Phys. Lett.* **29** 114216
[25] Hao Z H, Hu Z Y, Zhang J J, Hao Q Y and Zhao Y 2011 *Acta Phys. Sin.* **60** 117106 (in Chinese)
[26] Li R H, Meng W M, Peng Y Q, Ma C Z, Wang R S, Xie H W and Wang Y 2010 *Chin. Phys. Lett.* **27** 088401
[27] Liu X D, Zhao S L, Xu Z, Zhang F J, Zhang T H, Gong W, Yan G, Kong C, Wang Y S and Xu X R 2011 *Chin. Phys. B* **20** 068801
[28] Guo Y, Liu C, Tanaka H and Nakamura E 2015 *J. Phys. Chem. Lett.* **6** 535
[29] Liu X, Yu D, Cao F, Li X, Ji J, Chen J, Song X and Zeng H 2017 *Small* **13** 1700364
[30] Dong H, Zhu H, Meng Q, Gong X and Hu W 2012 *Chem. Soc. Rev.* **41** 1754
[31] Dou L, Liu Y, Hong Z, Li G and Yang Y 2015 *Chem. Rev.* **115** 12633
[32] Mishra A and Bäuerle P 2004 *Angew. Chem.* **43** 2020
[33] Chen X, Liu X, Wu B, Nan H, Guo H, Ni Z, Wang F, Wang X, Shi Y and Wang X 2017 *Nano Lett.* **17** 6391
[34] Hiramoto M, Imahigashi T and Yohoyama M 1994 *Appl. Phys. Lett.* **64** 187
[35] Nakayama K I, Hiramoto M and Yokoyama M 1998 *J. Appl. Phys.* **84** 6154
[36] Hiramoto M, Kawase S and Yokoyama M 1996 *Jpn. J. Appl. Phys.* **35** 349
[37] Katsume T, Hiramoto M and Yohoyama M 1996 *Appl. Phys. Lett.* **69** 3722
[38] Bao W, Cai X, Kim D, Sridhara K and Fuhrer M S 2013 *Appl. Phys. Lett.* **102** 042104
[39] Yao Y, Liang Y, Shrotriya V, Xiao S, Yu L and Yang Y 2007 *Adv. Mater.* **19** 3979
[40] Wang X, Li H, Su Z, Fang F, Zhang G, Wang J, Chu B, Fang X, Wei Z, Li B and Li W 2014 *Org. Electron.* **15** 2367
[41] Zhang T, Chu B, Li W, Su Z, Peng Q M, Zhao B, Luo Y, Jin F, Yan X, Gao Y, Wu H, Zhang F, Fan D and Wang J 2015 *ACS Appl. Mater. Interfaces* **7** 2529
[42] Zimmerman J D, Diev V V, Hanson K, Lunt R R, Yu E K, Thompson M E and Forrest S R 2010 *Adv. Mater.* **22** 2780
[43] Qi J, Ni L, Yang D, Zhou X, Qiao W, Li M, Ma D and Wang Z Y 2014 *J. Mater. Chem. C* **2** 2431
[44] Peumans P, Bulovic V and Forrest S R 2000 *Appl. Phys. Lett.* **76** 3855
[45] Lee J, Jadhav P and Baldo M A 2009 *Appl. Phys. Lett.* **95** 192
[46] Yu G, Gao J, Hummelen J C, Wudl F and Heeger A J 1995 *Science* **270** 1789
[47] Halls J J M, Walsh C A, Greenham N C, Marseglia E A, Friend R H, Moratti S C and Holmes A B 1995 *Nature* **376** 498
[48] Spanggaard H and Krebs F C 2004 *Sol. Energy Mater. Sol. Cells* **83** 125
[49] Günes S, Neugebauer H and Sariciftci N S 2007 *Chem. Rev.* **107** 1324
[50] Cheng Y J, Yang S H and Hsu C S 2009 *Chem. Rev.* **109** 5868
[51] Li G, Shrotriya V, Huang J, Yao Y, Moriarty T, Emery K and Yang Y 200 5 *Nat. Mater.* **4** 864
[52] Chen H Y, Hou J, Zhang S, Liang Y, Y ang G, Yang Y, Yu L, Wu Y and Li G 2009 *Nat. Photon.* **3** 649
[53] Huo L, Hou J, Zhang S, Chen H Y and Yang Y 2010 *Angew. Chem.* **122** 1542 2010 *Angew. Chem. Int. Ed.* **49** 1500
[54] Liang Y, Xu Z, Xia J, Tsai S T, Wu Y, Li G, Ray C and Yu L 2010 *Adv. Mater.* **22** E135
[55] Kojima A, Teshima K, Shirai Y and Miyasaka T 2009 *J. Am. Chem. Soc.* **131** 6050
[56] Dong R, Fan Y, Chae J, Dai J, Xiao Z, Dong Q, Yuan Y, Centrone A, Zeng X C and Huang J 2015 *Adv. Mater.* **27** 1912
[57] Hu X, Zhang X, Liang L, Bao J, Li S, Yang W and Xie Y 2014 *Adv. Funct. Mater.* **24** 7373
[58] Dou L, Yang Y, You J, Hong Z, Chang W H , Li G and Yang Y 2014 *Nat. Commun.* **5** 5404
[59] Gasparini N, Gregori A, Salvador M, Biele M, Wadsworth A, Tedde S, Baran D, McCulloch I and Brabec C J *Adv. Mater. Technol.* **3** 1800104

[60] Wang X, Wang H, Zhou D, Jin H and Yu J 2018 *Mater. Lett.* **230** 289
[61] Zhan X, Tan Z, Domercq B, An Z, Zhang X, Barlow S, Li Y, Zhu D, Kippelen B and Marder S 2007 *J. Am. Chem. Soc.* **129** 7246
[62] Few S, Frost J M, Kirkpatrick J and Nelson J 2014 *J. Phys. Chem. C* **118** 8253
[63] Guo X, Facchetti A and Marks T J 2014 *Chem. Rev.* **114** 8943
[64] Jiang W, Li Y and Wang Z 2014 *Acc. Chem. Res.* **47** 3135
[65] Nielsen C B, Holliday S, Chen H Y, Cryer S J and McCulloch I 2015 *Acc. Chem. Res.* **48** 2803
[66] Kang H, Lee W, Oh J, Kim T, Lee C and Kim B J 2016 *Acc. Chem. Res.* **49** 2424
[67] Diao Y, Zhou Y, Kurosawa T, Shaw Leo, Wang C, Park S, Guo Y, Reinspach J A, Gu K, Gu X, Tee B C K, Pang C, Yan H, Zhao D, Toney M F, Mannsfeld S C B and Bao Z 2015 *Nat. Commun.* **6** 7955
[68] Liu Z, Wu Y, Zhang Q and Gao X 2016 *J. Mater. Chem. A* **4** 17604
[69] Fernandez L F, Zink L N and Sastre Sa A 2016 *J. Mater. Chem. A* **4** 9336
[70] Buscema M, Isl, J O, Groenendijk D J, Blanter S I, Steele G A, Zant H S and Castellanos-Gomez A 2015 *Chem. Soc. Rev.* **44** 3691
[71] Wang J, Fang H, Wang X, Chen X, Lu W and Hu W 2017 *Small* **13** 1700894
[72] Fang H and Hu W 2017 *Adv. Sci.* **4** 1700323
[73] Liu X, Luo X, Nan H, Guo H, Wang P, Zhang L, Zhou M, Yang Z, Shi Y, Hu W, Ni Z, Qiu T, Yu Z, Xu J B and Wang X 2016 *Adv. Mater.* **28** 5200
[74] Kitazawa N, Watanabe Y and Nakamura Y 2002 *J. Mater. Sci.* **37** 3585
[75] Burschka J, Pellet N, Moon S J, Humphry B R, Gao P, Nazeeruddin M K and Grätzel M 2013 *Nature* **499** 316
[76] Lee Y, Kwon J, Hwang E, Ra C H, Yoo W J, Ahn J H, Park J H and Cho J H 2015 *Adv. Mater.* **27** 41
[77] Saran R and Curry R J 2016 *Nat. Photon.* **10** 81
[78] Pan R, Li H, Wang J, Jin X, Li Q, Wu Z, Gou J, Jiang Y and Song Y 2018 *Part. Part. Syst. Charact.* **35** 1700304
[79] Chang P H, Tsai Y C, Shen S W, Liu S Y, Huang K Y, Li C S, Chang H P and Wu C I 2017 *ACS Photon.* **4** 2335
[80] Chen S Y, Lu Y Y, Shih F Y, Ho P H, Chen Y F, Chen C W, Chen Y T and Wang W H 2013 *Carbon* **63** 23
[81] Jones G F, Pinto R M, Sanctis A D, Nagareddy V K, Wright C D, Alves H, Craciun M F and Russo S 2017 *Adv. Mater.* **29** 1702993
[82] Wang X, Wang P, Wang J, Hu W, Zhou X, Guo N, Huang H, Sun S, Shen H, Lin T, Tang M, Liao L, Jiang A, Sun J, Meng X, Chen X, Lu W and Chu J 2015 *Adv. Mater.* **27** 6575
[83] Tan W C , Shih W H and Chen Y F 2014 *Adv. Funct. Mater.* **24** 6818
[84] Yu S H, Lee Y, Jang S K, Kang J, Jeon J, Lee C, Lee J Y, Kim H, Hwang E, Lee S and Cho J H 2014 *ACS Nano* **8** 8285
[85] Xie C and Yan F 2017 *ACS Appl. Mater. Interfaces* **9** 1569
[86] Peng Z Y, Xu J L, Zhang J Y, Gao X and Wang S D 2018 *Adv. Mater. Interfaces* 1800505
[87] Qin L, Wu L, Kattel B, Li C, Zhang Y, Hou Y, Wu J and Chan W L 2017 *Adv. Funct. Mater.* **27** 47
[88] Han J, Wang J, Yang M, Kong X, Chen X, Huang Z, Guo H, Gou J, Tao S, Liu Z, Wu Z, Jiang Y and Wang X 2018 *Adv. Mater.*
[89] Taniyasu Y, Kasu M and Makimoto T 2006 *Nature* **441** 325
[90] Cho A Y and Arthur J R 1975 *Prog. Solid State Chem.* **10** 157
[91] Geim A K and Grigorieva I V 2013 *Nature* **499** 419
[92] Hong X, Kim J, Shi S F, Zhang Y, Jin C, Sun Y, Tongay S, Wu J, Zhang Y and Wang F 2014 *Nat. Nanotechnol.* **9** 682
[93] Britnell L, Ribeiro R M, Eckmann A, Jalil R, Belle B D, Mishchenko A, Kim Y J, Gorbachev R V, Georgiou T, Morozov S V, Grigorenko A N, Geim A K, Casiraghi C, Castro Neto A H and Novoselov K S 2013 *Science* **340** 1311
[94] Zhu H F, Li T, Zhang Y J, Dong H L, Song J S D, Zhao H P, Wei Z M, Xu W, Hu W P and Bo Z S 2010 *Adv. Mater.* **22** 1645
[95] Cheng R, Li D, Zhou H, Wang C, Yin A, Jiang S, Liu Y, Chen Y, Huang Y and Duan X 2014 *Nano Lett.* **14** 5590
[96] Furchi M M, Pospischil A, Libisch F, Burgdörfer J and Mueller T 2014 *Nano Lett.* **14** 4785
[97] Deng Y, Luo Z, Conrad N J, Liu H, Gong Y, Namjmaei S, Ajayan P, Lou J, Xu X and Ye P D 2014 *ACS Nano.* **8** 8292
[98] Jariwala D, Sangwan V K, Wu C C, Prabhumirashi P L, Geier M L, Marks T J, Lauhon L J and Hersam M C 2013 *Proc. Natl. Acad. Sci. U. S. A* **110** 18076
[99] Liu Y, Wang F, Wang X, Wang X, Flahaut E, Liu X, Li Y, Wang X, Xu Y, Shi Y, Zhang R 2015 *Nat. Commun.* **6** 9589
[100] Ye Y, Ye Z, Gharghi M, Zhu H, Zhao M, Wang Y, Yin X and Zhang X 2014 *Appl. Phys. Lett.* **104** 193508
[101] Yang H, Heo J, Park S, Song H J, Seo D H, Byun K E, Kim P, Yoo I, Chung H J and Kim K 2012 *Science* **336** 1140
[102] Vélez S, Ciudad D, Isl, J, Buscema M, Txoperena O, Parui S, Steele G A, Casanova F, Zant H S J, Castellanos G A and Hueso L E 2015 *Nanoscale* **7** 15442
[103] Liu F, Chow W L, He X, Hu P, Zheng S, Wang X, Zhou J, Fu Q, Fu W, Yu P, Zeng Q, Fan H J, Tay B K, Kloc C and Liu Z 2015 *Adv. Funct. Mater.* **25** 5865
[104] Jariwala D, Howell S L, Chen K S, Kang J, Sangwan V K, Filippone S A, Turrisi R, Marks T J, Lauhon L J and Hersam M C 2016 *Nano Lett.* **16** 497
[105] Radisavljevic B, Radenovic A, Brivio J, Giacometti V and Kis A 2011 *Nat. Nanotechnol.* **6** 147
[106] Lembke D, Bertolazzi S and Kis A 2015 *Acc. Chem. Res.* **48** 100
[107] Huang Y, Zhuge F, Hou J, Lv Liang, Luo Peng, Zhou Nan, Gan L and Zhai T 2018 *ACS Nano* **12** 4062
[108] Wang J, Yao Q, Huang C W, Zou X, Liao L, Chen S, Fan Z, Zhang K, Wu W, Xiao X, Jiang C and Wu W W 2016 *Adv. Mater.* **28** 8302
[109] Velusamy D B, Haque M A, Parida M R, Zhang F, Tom W, Mohammed O F and Alshareef H N 2017 *Adv. Funct. Mater.* **27** 1605554
[110] Haynes C L and Duyne R P V 2001 *J. Phys. Chem. B* **105** 5599
[111] Zhang J, Li Y, Zhang X and Yang B 2010 *Adv. Mater.* **22** 4249
[112] Chen Z, Li X, Wang J, Tao L, Long M, Liang S J, Ang L K, Shu C, Tsang H K and Xu J B 2017 *ACS Nano* **11** 430
[113] Petoukhoff C E, Krishna M B M, Voiry D, Bozkurt I, Deckoff-Jones S, Chhowalla M, O'Carroll D M and Dani K M 2016 *ACS Nano* **10** 9899
[114] Kim J S, Kim B J, Choi Y J, Lee M H, Kang M S and Cho J H 2016 *Adv. Mater.* **28** 4803
[115] Kim J S, Choi Y J, Woo H J, Yang J, Song Y J, Kang M S and Cho J H 2017 *Adv. Funct. Mater.* **27** 1704475
[116] Liu Z, Parvez K, Li R, Dong R, Feng X and Müllen K 2015 *Adv. Mater.* **27** 669
[117] Pang S, Yang S, Feng X and Müllen K 2012 *Adv. Mater.* **24** 1566
[118] Wang X, Song W, Liu B, Chen G, Chen D, Zhou C and Shen G 2013 *Adv. Funct. Mater.* **23** 1202